PHOTONIC SENSORS / Vol. 7, No. 1, 2017: 48–54

# Acoustic Emission Localization Based on FBG Sensing Network and SVR Algorithm

Yaozhang SAI[1*], Xiuxia ZHAO[2], Dianli HOU[1], and Mingshun JIANG[3]

[1]*School of Information and Electrical Engineering, Ludong University, Yantai, 264025, China*

[2]*TIANRUN CRANKSHAFT CO., LTD, Wendeng, 264400, China*

[3]*School of Control Science and Engineering, Shandong University, Jinan, 250061, China*

[*]Correspond author: Yaozhang SAI E-mail: saiyaozhang@163.com

**Abstract:** In practical application, carbon fiber reinforced plastics (CFRP) structures are easy to appear all sorts of invisible damages. So the damages should be timely located and detected for the safety of CFPR structures. In this paper, an acoustic emission (AE) localization system based on fiber Bragg grating (FBG) sensing network and support vector regression (SVR) is proposed for damage localization. AE signals, which are caused by damage, are acquired by high speed FBG interrogation. According to the Shannon wavelet transform, time differences between AE signals are extracted for localization algorithm based on SVR. According to the SVR model, the coordinate of AE source can be accurately predicted without wave velocity. The FBG system and localization algorithm are verified on a 500 mm×500 mm×2 mm CFRP plate. The experimental results show that the average error of localization system is 2.8 mm and the training time is 0.07 s.

**Keywords:** Fiber Bragg grating; acoustic emission localization; support vector regression; carbon fiber reinforced plastics

Citation: Yaozhang SAI, Xiuxia ZHAO, Dianli HOU, and Mingshun JIANG, "Acoustic Emission Localization Based on FBG Sensing Network and SVR Algorithm," *Photonic Sensors*, 2017, 7(1): 48–54.

## 1. Introduction

Carbon fiber reinforced plastics (CFRP) have been widely applied in aircraft industry [1, 2]. But due to the impact and material fatigue, various barely visible damages can appear [3, 4]. The damages seriously degrade the reliability of CFRP structure and affect structure safety [5, 6]. Due to above reasons, damages should be timely located. The acoustic emission (AE) technology is an important damage detection means with great potential. Various damages of CFRP can cause AE phenomenon. According to the AE source localization, we can determine the location of damages.

Due to weight and size, the traditional AE piezoelectric sensor is difficult for damages detection of aircraft. In recent years, the fiber Bragg grating (FBG) sensor is researched for detecting AE signals [7, 8]. Because of light weight and small size of the FBG, it is appropriate for the AE detection in aircraft. Many methods are researched for the AE localization. Lu *et al*. [9] used the particle swarm optimization (PSO) algorithm to achieve the AE localization in an aluminum alloy plate. The localization error is less than 10mm. But the algorithm is not appropriate for the AE localization of anisotropic materials. Mostafapour *et al*. [10] developed a wavelet transform and cross-time frequency spectrum technology for the AE source

Received: 26 September 2016 / Revised: 30 September 2016

DOI: 10.1007/s13320-016-0377-x
Article type: Regular

localization, and high localization accuracy was obtained. Wave velocity is necessary for this technology. Therefore, it is only appropriate for the AE localization of an isotropic plate on which wave velocity is easily acquired. Fu *et al*. [11] used the back propagation neural network to realize the AE localization. But the algorithm uses wave velocity which is difficult to be obtained in the CFRP structure. Xiao *et al*. [12] applied the beamforming method to locate AE source in the CFRP plate. However, the wave velocity is still necessary. Jiang *et al*. [13] applied least squares support vector machine for the AE localization without wave velocity. The average localization error was 6.78 mm. But the frequency dispersion, which seriously affects the localization accuracy, is not been considered. Kim *et al*. [14] used the least squares support vector machine (LSSVM) to locate AE source, and better localization accuracy was obtained. However, the method is only used in an aluminum alloy plate.

In this paper, an FBG sensing network and support vector regression (SVR) algorithm are developed for the AE source localization on the CFRP plate. A high-speed FBG interrogation system is designed to obtain AE signals. The Shannon wavelet transform is applied to extract narrow-band signals of AE signals for AE localization, which reduces the influence of frequency dispersion on the AE localization. According to time differences of narrow-band signals, the SVR algorithm, which does not use wave velocity, is applied to locate AE source with high accuracy. The FBG sensing system and localization algorithm are verified on the CFRP plate. The experimental results show that the localization system is practical and efficient.

## 2. Localization algorithm

In many AE localization methods of CFRP, wave velocity is necessary. However, the CFRP material is anisotropic. Wave velocities of different directions are difference. If wave velocity is used for localization, it must be accurately measured in different directions. However, the work is very difficult in practical applications. In this paper, we only use time differences of AE signals. The SVR algorithm is applied to forecast the coordinate of AE source.

### 2.1 Shannon wavelet transform

The frequency dispersion of AE wave and noise can seriously affect the calculation of time difference. Therefore, the Shannon wavelet transform is applied to extract narrow-band signals of AE signals for time differences.

Shannon wavelet transform can be expressed as

$$WT(x,a,b)=\frac{1}{\sqrt{a}}\int_{-\infty}^{+\infty}u(x,t)\psi^{*}\left(\frac{t-b}{a}\right)dt \quad (1)$$

where $a$ and $b$ are scale factor and time factor, respectively. $\psi(t)$ is the Shannon wavelet function which is given by

$$\psi(t)=\sqrt{f_b}\sin c(f_b t)e^{2\pi i f_c t} \quad (2)$$

where $f_b=\omega_b/2\pi$ and $f_c=\omega_c/2\pi$. The Fourier transform of the Shannon wavelet function is expressed as

$$\Psi(\omega)=\begin{cases}\sqrt{\dfrac{2\pi}{\omega_b}}, & \omega_c-\dfrac{\omega_b}{2}<\omega\le\omega_c+\dfrac{\omega_b}{2}\\ 0, & \text{others}\end{cases} \quad (3)$$

where $\Psi(\omega)$ is the rectangular window function of which the bandwidth and central frequency are $\omega_b$ and $\omega_c$, respectively [15]. The narrow-band signals can be obtained by the Shannon wavelet transform. The AE signal $u(x,t)$ can be defined as

$$u(x,t)=e^{-\mathrm{j}(k_1x-\omega_1t)}+e^{-\mathrm{j}(k_2x-\omega_2t)} \quad (4)$$

where $k_1$ and $k_2$ are wave numbers. Introduction:

$$\begin{aligned}&\Psi^{*}(a\omega)=\Psi^{*}(a\omega_1)=\Psi^{*}(a\omega_2)\\ &\frac{k_2-k_1}{2}=\Delta k,\ \frac{\omega_2-\omega_1}{2}=\Delta\omega\\ &\frac{k_1+k_2}{2}=k_0,\ \frac{\omega_1+\omega_2}{2}=\omega_0.\end{aligned} \quad (5)$$

After the Shannon wavelet transform, the module value of AE signals can be obtained as

$$\begin{aligned}&\left|WT(x,a,b)\right|=\\ &\sqrt{2a}\left|\Psi(a\omega_0)\right|\sqrt{1+\cos(\Delta\omega b-\Delta kx)}.\end{aligned} \quad (6)$$

When $b=\Delta k/\Delta\omega$, the module value is the maximum. The time differences of AE signals are obtained by the peak times of module values of narrow-band signals.

### 2.2 SVR model

The basic idea of the SVR model is to map low-dimensional data into high-dimensional feature space by using a nonlinear mapping function, then to perform linear regression in this space. Given a training set of data $G=\{(x_i, y_i)\}(i=1, 2, \cdots, N)$, where $x_i$ is an input vector, and $y_i$ is an expected value. In the AE localization, $x_i$ is a time differences vector of AE signals, and $y_i$ is the ordinate or the abscissa of AE source. The regression function is expressed as

$$f(x)=w\phi(x_i)+b \tag{7}$$

where $\phi(x_i)$ is a mapping function, $w$ is a weight vector, and $b$ is an error value. $w$ and $b$ are confirmed by minimizing the regularized risk function which is as follows:

$$\begin{aligned}&\min \frac{1}{2}\|w\|^2+C\frac{1}{N}\sum_{i=1}^{N}L\left[f(x_i)-y_i\right]\\&s.t.\quad L\left[f(x_i)-y_i\right]\\&=\begin{cases}\left|f(x_i)-y_i\right|-\varepsilon, & \left|f(x_i)-y_i\right|\geq\varepsilon\\0, & \left|f(x_i)-y_i\right|<\varepsilon\end{cases}\end{aligned} \tag{8}$$

where $C$ is a penalty factor, $L(\cdot)$ is an $\varepsilon$-non-sensitive loss function, and $\varepsilon$ is an $\varepsilon$-intensive loss parameter. Two relaxation factors $\xi_i$ and $\xi_i^*$, which control a linearly inseparable boundary, are introduced [16]. So (8) can be rewritten as

$$\begin{aligned}&\min_{w,b,\xi_i,\xi_i^*}\frac{1}{2}\|w\|^2+C\frac{1}{N}\sum_{i=1}^{N}(\xi_i+\xi_i^*)\\&s.t.\quad L\left[f(x_i)-y_i\right]\\&=\begin{cases}y_i-w\phi(x_i)-b\leq\varepsilon+\xi_i,\ \xi_i\geq 0\\w\phi(x_i)+b-y_i\leq\varepsilon+\xi_i^*,\ \xi_i^*\geq 0.\end{cases}\end{aligned} \tag{9}$$

By introducing Lagrangian multiplier $a_i$ and $a_i^*$, the above formula can be rewritten as

$$\begin{aligned}&\min_{a}\frac{1}{2}\sum_{i,j=1}^{N}(a_N^*-a_N)(a_j^*-a_j)K(x_i,x_j)+\\&\varepsilon\sum_{i=1}^{N}(a_i^*+a_i)-\sum_{i=1}^{N}(a_i^*-a_i)\end{aligned}$$

$$s.t.\begin{cases}w=\sum_{i=1}^{N}(a_i^*-a_i)x_i\\\sum_{i=1}^{N}(a_i^*-a_i)=0\\0\leq a_i^*,\ a_i\leq C\end{cases} \tag{10}$$

where $K(x_i, x_j)$ is a kernel function [17]. We use the radial basis function (RBF). The resulting regression function of SVR model can be expressed as

$$f(x)=\sum_{i=1}^{N}(a_i^*-a_i)K(x_i,\ x)+b\,. \tag{11}$$

The coordinate of AE source includes the ordinate and the abscissa, but the above SVR model can only output one valve. Two SVR models are built to respectively predict the ordinate and the abscissa of AE source.

### 2.3 AE localization process

The specific localization process, which is realized by the Shannon wavelet transform and SVR, is as follows:

(1) The coordinate, on which AE experiments are implemented and training data is obtained, is determined.

(2) AE experiments are implemented on training data points. AE signals are acquired. According to the Shannon wavelet transform, time differences of narrow-band signals of AE signals are extracted. Time differences and coordinates are used as training data.

(3) According to training data, SVR localization models, which output the ordinate and the abscissa of AE source, are built. According to cross validation, models are tested to confirm that models can be used for AE localization.

## 3. AE source localization

### 3.1 Experimental setup

AE localization experiments are implemented on a 300 mm×300 mm monitoring area of CFRP plate, whose dimension is 500 mm×500 mm×2 mm. Four FBG sensors are stuck on four corners of the CFRP

plate, respectively. The FBG interrogation system includes FBG sensors, tunable narrow-band laser, fiber-optic coupler, optical circulator, photoelectric converter, amplifier, and data acquisition system, as shown in Fig. 1. The sampling frequency of FBG interrogation system is 5 MHz. The reflectance wavelengths of all FBG sensors are close to 1565.213 nm and errors are less than 0.01 nm. When FBGs are stuck, a definite pretension force is applied to them. The central wavelength of tunable narrow-band laser is 1565.238 nm, and wavelength variation is less than ±1 pm. The output power is 1 mW. The wavelength of narrow-band light source lies in the linear edge of FBG reflectance spectrum. The narrow-band laser demodulation technology is applied to obtain AE signals [7]. AE signals are generated by steel ball impact. The AE localization system is shown in Fig. 2.

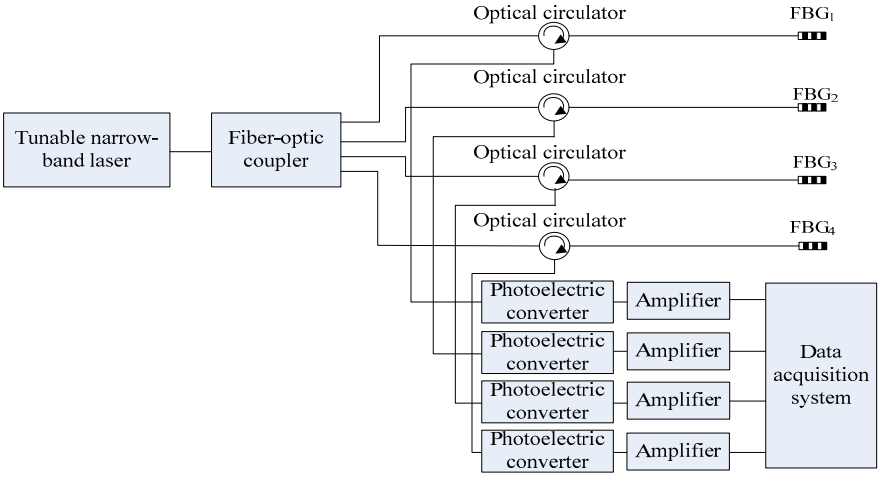


Fig. 1 FBG interrogation system.

### 3.2 AE localization experiment

The coordinates of four FBGs respectively are (0, 300), (300, 300), (300, 0) and (0, 0) in the monitoring area, as shown in Fig. 3. The monitoring area is divided into 36 small areas. Every small area is 50 mm×50 mm. The central point of a small area is chosen to carry out AE experiments and obtain AE experiments data for the training SVR model. The central point of big area, which is composed of four adjacent small areas, is chosen for testing data of the SVR model.

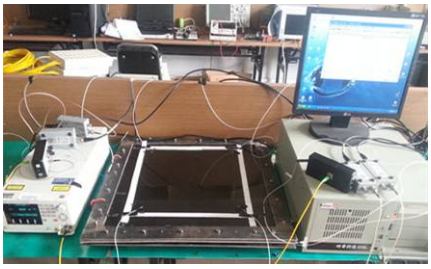

Fig. 2 AE localization experiment system.

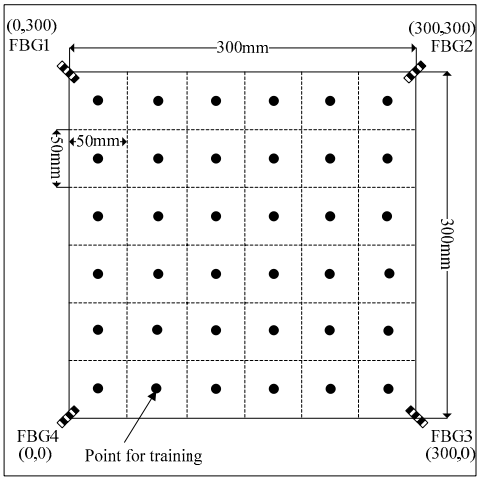


Fig. 3 AE experimental layout.

On the above points, AE experiments are implemented. AE signals are obtained by FBG sensors. AE signals, which are acquired by carrying out AE experiments on the closest point of $FBG_1$, are shown in Fig. 4. Figure 5 is the frequency spectrum of AE signals of $FBG_1$. According to the

frequency spectrum, the AE signal is a wideband signal. The frequency range is 20 kHz–200 kHz. According to frequency dispersion effect and signal attenuation, the accurate time differences between AE wide-band signals are difficult to be extracted. So AE narrowband signal, whose central frequency is 40 kHz, is extracted by the Shannon wavelet transform. At the same time, the module value of narrowband signal is calculated. According to the peaks of module values, time differences between AE signals can be obtained, as shown in Fig. 6. For the training SVR model, time differences between $FBG_1$ signals and other sensors signals are used for input, and the coordinates of points for training are used for output. According to the above process, SVR models for AE localization are built.

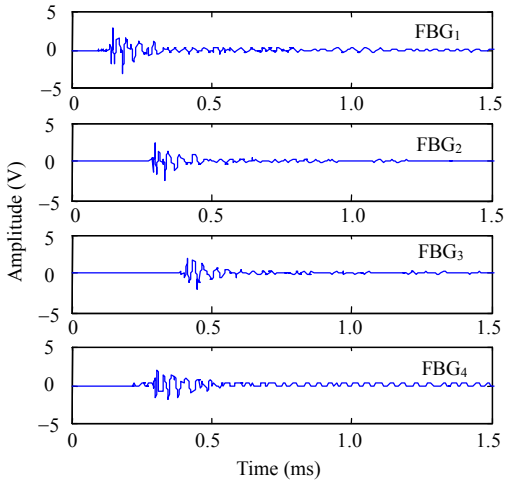


Fig. 4 AE signals.

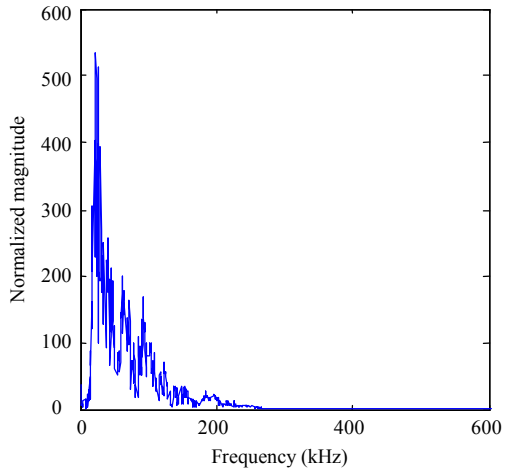


Fig. 5 Frequency spectrum of AE signals.

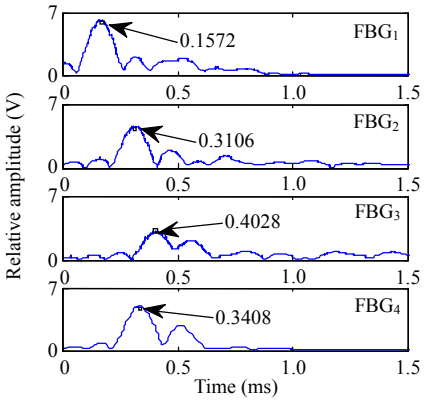


Fig. 6 Model values of narrowband signals.

For testing the SVR model for the AE localization, AE experiments are carried out on arbitrary ten testing points. Time differences are inputted, and the prediction coordinates of testing point are outputted. For making the contrast analysis of SVR and neural network, RBF neural network is applied for the AE localization. The testing results of SVR and RBF neural network are shown in Fig. 7. According to the radial error principle, the testing errors are calculated and shown in Fig. 8. The maximum errors of SVR and RBF are 7.2 mm and 6 mm, and the minimum errors are 0.4 mm and 0.8 mm, respectively. The average errors of SVR and RBF neural network are 2.8 mm and 3.7 mm, respectively. At the same time, the training times of SVR and RBF neural network are 0.07 s and 0.84 s, respectively. Compared with the RBF neural network, the localization accuracy of SVR is higher, and the training time is less. The above calculation results are given by MATLAB 7.1 and computer with AMD 3.0 GHz CPU.

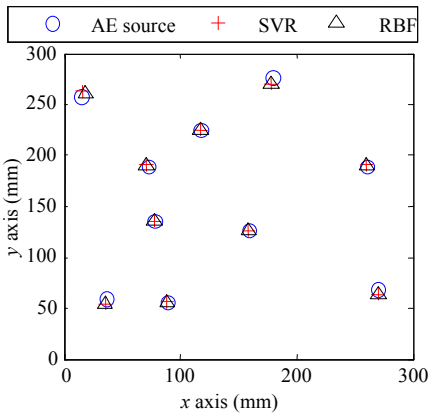


Fig. 7 Result of testing experiments.

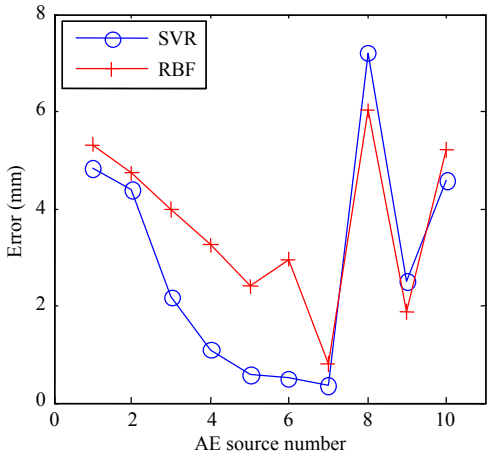


Fig. 8 Error of testing experiment.

## 4. Conclusions

In this paper, an AE localization system based on FBG sensing network and SVR algorithm is proposed. According to the narrowband laser demodulation technology, AE signals can be obtained by FBG sensors. The Shannon wavelet transform is applied for time differences between AE signals. According to time difference and SVR, the AE source is accurately located. The FBG system and localization algorithm are verified on the 500 mm×500 mm×2 mm CFRP plate. The average error of localization system is 2.8 mm, and training takes 0.07 s. Therefore, this paper proposes a practical AE localization system of CFRP plate for damage detection

## Acknowledgment

This research is supported by the National Natural Science Foundation of China (Grant Nos. 61503218 and 41472260), the Fundamental research funds of Shandong University, China under Grant Nos. 2014YQ009, 2016JC012, and the Young Scholars Program of Shandong University 2016WLJH30.



## References

[1] M. Grujicic, B. Pandurangan, W. C. Bell, C. F. Yen, and B. A. Cheeseman, "Application of a dynamic-mixture shock-wave model to the metal–matrix composite materials," *Materials Science and Engineering: A*, 2011, 528(28): 8187–8197.

[2] A. Katunin, K. Dragan, and M. Dziendzikowski, "Damage identification in aircraft composite structures: a case study using various non-destructive testing techniques," *Composite Structures*, 2015, 127(9): 1–9.

[3] F. Otero, S. Oller, S. X. Martinez, and O. Salomon, "Numerical homogenization for composite materials analysis. Comparison with other micro mechanical formulations," *Composite Structures*, 2015, 122(4): 405–416.

[4] H. Singh, K. K. Namala, and P. Mahajan, "A damage evolution study of E-glass/epoxy composite under low velocity impact," *Composites Part B: Engineering*, 2015, 76(8): 235–248.

[5] J. Zhang and X. Zhang, "An efficient approach for predicting low-velocity impact force and damage in composite laminates," *Composite Structures*, 2015, 130(12): 85–94.

[6] P. Yang, S. S. Shams, A. Slay, B. Brokate, and R. Elhajjar, "Evaluation of temperature effects on low velocity impact damage in composite sandwich panels with polymeric foam cores," *Composite Structures*, 2015, 129(11): 213–223.

[7] D. Pang and Q. Sui, "Response analysis of ultrasonic sensing system based on fiber Bragg gratings of different lengths," *Photonic Sensors*, 2014, 4(3): 281–288.

[8] Z. Jin, M. Jiang, Q. Sui, F. Zhang, and L. Jia, "Acoustic emission source linear localization based on an ultra-short FBGs sensing system," *Photonic Sensors*, 2014, 4(2):152–155.

[9] S. Lu, M. Jiang, Q. Sui, H. Dong, Y. Sai, and L. Jia, "Acoustic emission location on aluminum alloy structure by using FBG sensors and PSO method," *Journal of Modern Optics*, 2015, 63(8):1–8.

[10] A. Mostafapour, S. Davoodi, and M. Ghareaghaji, "Acoustic emission source location in plates using wavelet analysis and cross time frequency spectrum," *Ultrasonics*, 2014, 54(8): 2055–2062.

[11] T. Fu, Z. Zhang, Y. Liu, and J. Leng, "Development of an artificial neural network for source localization using a fiber optic acoustic emission sensor array," *Structural Health Monitoring*, 2015, 14(2): 168–177.

[12] D. Xiao, T. He, Q. Pan, X. Liu, J. Wang, and Y. Shan, "A novel acoustic emission beamforming method with two uniform linear arrays on plate-like structures," *Ultrasonics*, 2014, 54(2): 737–745.

[13] M. Jiang, S. Lu, Y. Sai, Q. Sui, and L. Jia, "Acoustic emission source localization technique based on least squares support vector machine by using FBG sensors," *Journal of Modern Optics*, 2014, 61(20): 1634–1640.

[14] K. Kim and Y. Lee, "Acoustic emission source localization in plate-like structures using least-squares support vector machines with delta t feature," *Journal of Mechanical Science and Technology*, 2014, 28(8): 3013–3020.

[15] Y. Sai, M. Jiang, Q. Sui, S. Lu, and L. Jia, "Multi-source acoustic emission localization technology research based on FBG sensing network and time reversal focusing imaging," *Optik*, 2016, 127(1): 493–498.

[16] Y. Liu and R. Wang, "Study on network traffic forecast model of SVR optimized by GAFSA," *Chaos, Solitons and Fractals*, 2016, 89(3): 153–159.

[17] W. Zhang, W. Hong, Y. Dong, G. Tsai, J. Sung, and G. Fan, "Application of SVR with chaotic GASA algorithm in cyclic electric load forecasting," *Energy*, 2012, 45(1): 850–858.